THE PREPARATION AND CHARACTERIZATION OF Fe_2O_3 / FTO GAS SENSOR TO SENSEING CARBON MONOXIDE GAS CO

Hussein Mohammed Talib(a), Mehmet Ali Yıldırım(b),

Department of Electrical and Electronic Engineering, Engineering Faculty, Erzincan University, Turkey (a)

Department of Electrical and Electronic Engineering, Engineering Faculty, Erzincan University, Turkey (b)

mohhussein358@gmail.com

ABSTRACT:

In this study, Fe_2O_3 thin film was successfully grown on fluorine doped tin oxide (FTO) coated glass substrate at 30 SILAR cycles at room temperature by the Successive Ionic Layer Adsorption and Reaction (SILAR) method. The structural, morphological, chemical composition and CO gas sensing properties of the thin film were investigated by XRD, SEM, EDAX and gas measurement system, respectively. XRD and SEM studies indicated that the thin film had polycrystalline nature and was crystallized in the hematite (α-Fe_2O_3) phase, there were dense coating and regional agglomerations of different sizes on the FTO substrate surface. EDAX analysis confirmed the presence of Fe and O elements and formation of iron oxide on the surface of the film. Static and dynamic CO gas detection measurements of the Fe_2O_3/FTO sensor were done. It was observed that the sensitivity of the sensor increased with the operating temperature up to 285 °C and the optimum operating temperature was 285 °C. At operating temperature of 285 °C, the sensitivity value of the sensor was determined as 10% for 5 ppm CO gas and 47.8% for 100 ppm CO gas. The response and recovery times of the sensor were calculated. In addition, the repeatability, stability and selectivity measurements for the control group gases were done.

Keywords: (CO gas, Gas sensors, Iron oxide, Metal oxide thin films).

1. INTRODUCTION

Many toxic gases exist in the atmosphere; for example, carbon monoxide (CO), a major air pollutant that results from the burning of fossil fuels, car exhaust, and emissions from industrial factories. CO poisoning results in >5000 deaths per year in the USA. In Denmark, from 1995 to 2015, there were several hundred fatalities due to CO poisoning.

Additionally, in Iran, a developing country, approximately 836 deaths occurred in 2016 due to CO poisoning. CO is a tasteless, colorless, and odorless gas that has 240 times greater affinity for hemoglobin compared with O_2. It forms carboxyhemoglobin, which leads to reduced O_2 delivery to tissues and can cause tissue hypoxia. Additionally, CO easily binds to cytochrome oxidase and leads to lactic acidosis, apoptosis, and hypoxia [1] (Mirzaei et al., 2019). However, different gas sensor technologies have been used for the detection of different gases for centuries, including semiconductor gas sensors, optical gas sensors, catalytic gas sensors, acoustic gas sensors, and electrochemical gas sensors. The performance characteristic of each sensor is based on some characteristics such as sensitivity, selectivity, detection limit, response time and recovery time [2] (Pearton et al., 2010). Many scientists and engineers have studied metal oxide thin films as electronic materials because of their semiconductor behavior, structural simplicity and low cost. Widely known iron oxide thin films include FeO, Fe_3O_4 and Fe_2O_3, among which Fe_2O_3 possess high chemical stability and nontoxicity. Due to the excellent optical, electrical, and magnetic properties, Fe_2O_3 thin film has been widely adopted in the functional fields, e.g., photocatalysis, gas sensing, and capacitive device. Fe_2O_3 exists in two distinct atomic structures namely the α-Fe_2O_3 and γ-Fe_2O_3, which belongs to hexagonal and cubic crystal system, respectively. Furthermore, α-Fe_2O_3 is antiferromagnetic whereas γ-Fe_2O_3 is ferromagnetic. In comparison to γ-Fe_2O_3, α-Fe_2O_3 is more stable and has more applications in various fields [3] (Ma et al., 2021). Metal oxide gas sensors are among most important devices to detect a large variety of gases. α-Fe_2O_3, an environmental friendly semiconductor ($E_g = 2.1$ eV), is the most stable iron oxide under ambient atmosphere and because of its low cost, high stability, high resistance to corrosion, and its environmentally friendly properties is one of the most important metal oxides for gas sensing applications [4] (Mirzaei et al., 2016). Since iron (III) oxide has all these good properties, it is a promising material in photovoltaic and electrical applications and devices in addition to photocatalytic applications and sensors. This artıcle study includes the growth of Fe_2O_3

thin film on fluorine doped tin oxide (FTO) substrates by Successive Ionic Layer Adsorption And Reaction (SILAR) method and examining the structural, morphological, chemical component and CO gas detection properties of this film.

2. EXPERIMENTAL DETAILS

The glass substrate materials were cut to 9 mm wide and 25 mm long. Fe_2O_3 thin films were deposited by SILAR method on glass substrates.

In this study, Fe_2O_3 thin films were deposited on glass substrates using SILAR method at room temperature and ambient pressure. To deposit Fe_2O_3 thin film, aqueous iron-ammonia complex ions ($[Fe(NH_3)^4]^3+$) were chosen for the cation precursor. To prepare the iron-amanioc complex, 25-28% NH_4OH solution was added to 0.1M $FeCl_3$ (pH ≈ 5.5) solution, making the pH of the solution ≈ 10. The Fe_2O_3 thin film growth mechanism with the SILAR method is shown in Figure 2.1. To prepare Fe_2O_3 thin film, 30 SILAR preparation cycle involves the four following steps: (1) immersing the substrate in the precursor solution for 25 s to create a thin liquid film containing $[Fe(NH_3)_4]^3+$ on the substrate; (2) immersing immediately the withdrawn substrates in hot water (~ 90 ^oC) for 7 s to form Fe_2O_3 layer; (3) drying the substrate in the air for 60 s; and (4) rinsing the substrate in a separate beaker for 20 s to remove large and loosely bonded Fe_2O_3 particles. All steps are carried out at room temperature. Thus, one SILAR cycle of nanostructure Fe_2O_3 thin film preparation was completed. The Fe_2O_3 film was prepared by repeating 30 SILAR cycles.

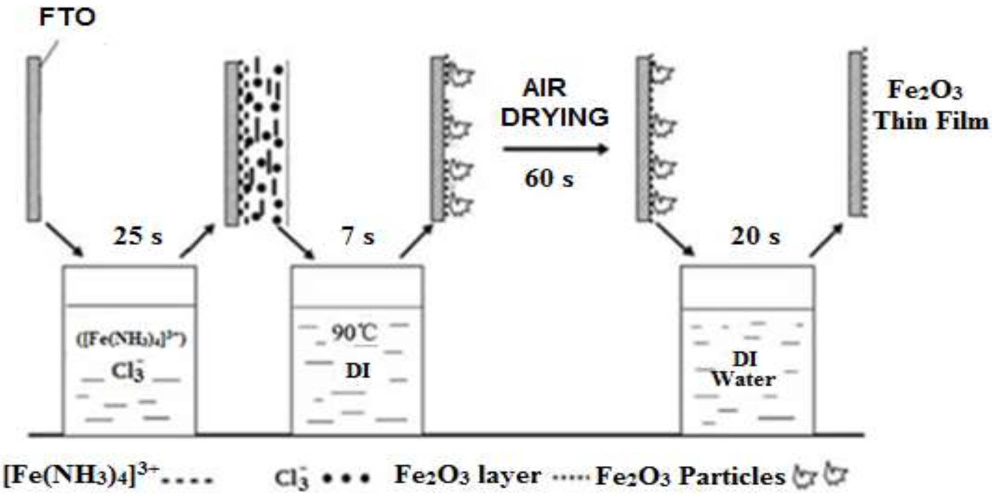

Figure 2.1. Growth of Fe_2O_3 thin films by SILAR method

Firstly, structural, morphological and elemental characterizations of the Fe_2O_3 thin film were carried out. After then, the inter digitated (IDT) silver electrodes were coated on the thin film by thermal evaporation. Finally, gas sensing measurements were tested for this structure, where the Structure of Fe_2O_3 thin film is shown in Figure 2.2

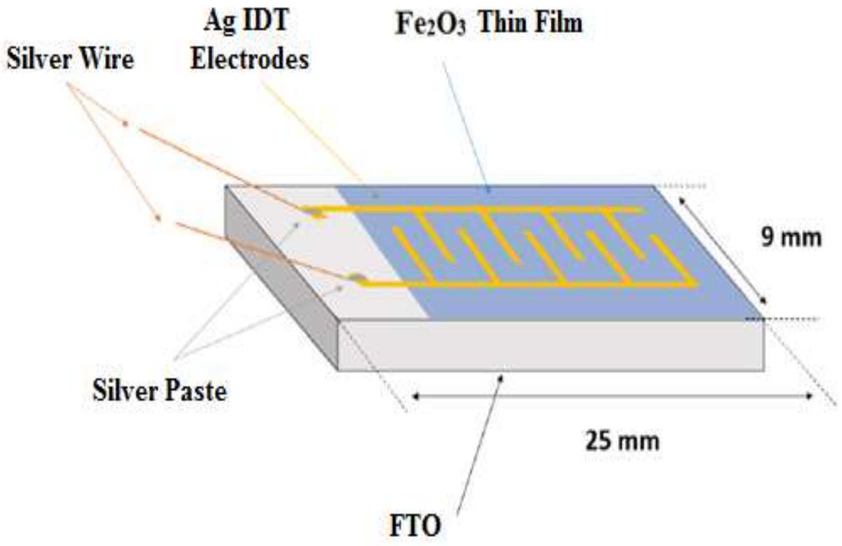

Figure 2.2. Schematic diagram of Fe_2O_3/FTO gas sensor

The gas sensing properties of the Fe_2O_3 thin film sensors were tested using a special computer-controlled measurement system [5]

3. RESULTS AND DISCUSSION

X-ray Diffraction patterns of the α-Fe_2O_3 thin film was recorded using Panalytical Empyrean X-ray diffractometer with Cu-Kα radiation (λ=1,5405 Å) with 2θ of 20^o -80^o , operated at 45 kV and 40 mA. XRD analysis was used in the present work to identify the crystalline phases and the structural properties of the obtained thin film from SILAR deposition process. Fig 3.1 shows the XRD patterns of obtained α-Fe_2O_3 thin film.

Crystallinity refers to the degree of structural order in a solid.

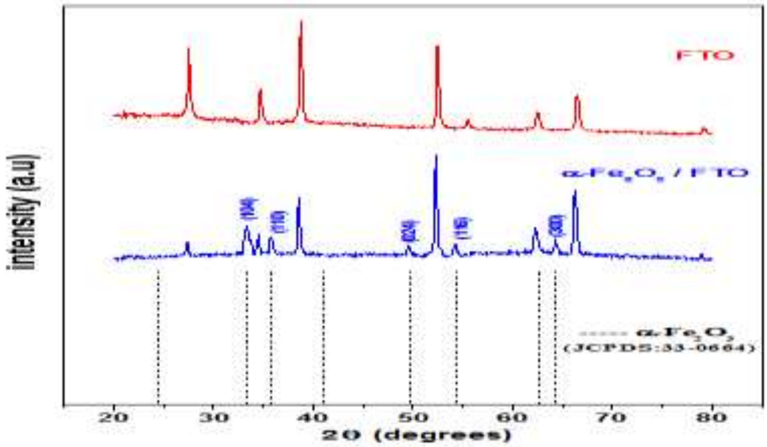

Figure 3.1. X-ray diffraction pattern of Fe_2O_3 thin film with 30 SILAR cycles

The diffraction peaks of the XRD pattern matches with the rhombohedral crystalline structure of Hematite phase (JCPDS Card No: 33-0664). The peaks were indexed as (104), (110), (024), (116), and (300) of rhombohedral α-Fe_2O_3 [6],[7],[8],[3],[9] (Sheik Fareed et al., 2018; Khakpour et al., 2018; Rahman et al., 2020; Ma et al., 2021; Machreki et al., 2021).

Using the XRD diffraction measurements given in Figure 3.1, equations (3.1) and (3.2), the average crystal size and average dislocation density values of the α-Fe_2O_3 thin film are given in Table 3.1.

$$\boldsymbol{D = (k\,.\,\lambda) \,/\, (\beta\,.\,Cos\,(\theta))} \qquad \textbf{(3.1)}$$

where D, λ, β and θ are the average crystal size, the X-ray wavelength used, FWHM and Bragg's diffraction angle respectively. Additionally, to have more information on the amount of defects in the thin films, the dislocation density (**δ**) was evaluated by using the formula below [99/18/Mns yildirim],

$$\delta = \frac{n}{D^2} \tag{3.2}$$

Table 3.1. Average crystal size (Davg) and mean dislocation density (δavg) values of α-Fe_2O_3 thin film

α-Fe_2O_3	**D_{avg} (nm)**	**δavg X 10^{-3} (nm^{-2})**
30 SILAR Cycle	22.4698	1.98

To investigate the morphological properties of the Fe_2O_3 thin film grown by the SILAR method, the SEM image of the film was taken using the FEI Quanta FEG 450 model Environmental Scanning Electron Microscope (FESEM) device. The SEM image of α-Fe_2O_3 thin film grown on FTO substrate in 30 SILAR cycle at 50,000 magnification is given in Figure 3.2.

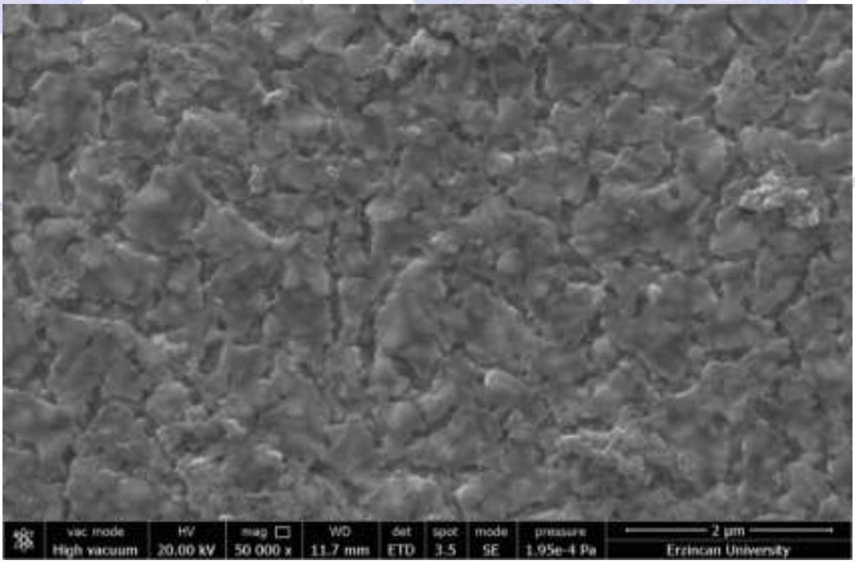

Figure 3.2. SEM image of Fe_2O_3 thin film with 30 SILAR cycle

From the SEM image, it has been observed that there is a dense layering and regional agglomerations of different sizes on the surface of the FTO substrate. In addition to that there are partial gaps between the agglomerations and these agglomerations are approximately homogeneously distribution on the FTO substrate. [10] (Choi et al., 2020).

For the elemental analysis of the Fe_2O_3 thin film grown with the SILAR method, Energy Dispersive X-ray Spectroscopy (EDAX) measurement of the film was taken. EDAX analysis of Fe_2O_3 thin film grown on FTO substrate is given in Figure 3.3.

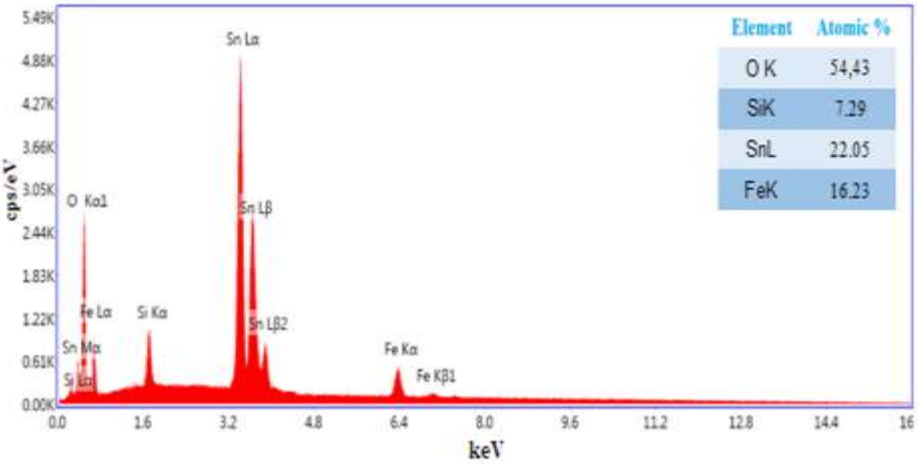

Figure 3.3. EDAX analysis of Fe_2O_3 thin film with 30 SILAR cycle

To obtain information about the chemical component of the Fe_2O_3 film, the EDAX analysis showed the presence of Fe and O elements on the surface of the film and confirmed the formation of iron oxide. In addition, the Si and Sn peaks are thought to originate from the FTO substrate used [11],[9] (Junior et al., 2021; Machreki et al., 2021).

After structural, morphological and elemental measurements of the Fe_2O_3 thin film grown with the SILAR method were made, static and dynamic gas measurements depending on temperature and gas concentration were carried out in the sensor measurement laboratory to characterize the CO gas detection properties of the Fe_2O_3/FTO sensor. The sensor response was calculated using the following relation;

$$\mathbf{S}\ (\%) = \frac{\mathbf{Rg - Ra}}{\mathbf{Ra}} * \mathbf{100} \qquad \mathbf{(3.3)}$$

where Ra and Rg are the resistivity in dry air and upon exposure the target gas in dry air, .respectively.

CO Gas Detection Results of Fe_2O_3 Thin Film Gas Sensors

(i). Static Gas Detection Results Based on Temperature

The operating temperature of the gas sensor is one of the main factors in examining the properties of the sensor. It is important to increase the temperature to achieve surface precise interactions on the surface of the sensor material. However, although important, very high temperatures can deteriorate the material structure and affect the life and operation of the sensor. Therefore, it is important to determine the optimum operating temperature of the sensor. To determine the CO gas detection properties of the Fe_2O_3/FTO gas sensor, the optimum operating temperature must first be determined. To find the optimum operating temperature, static gas measurements of the sensor were carried out at a constant 100 ppm CO gas concentration between room temperature and 360 °C. Static gas measurement of the Fe_2O_3/FTO sensor is given in Figure 3.4. As seen in Figure 3.4, it was determined that the sensor was sensitive to 100 ppm CO gas starting from 90 ^{o}C. The optimum operating temperature for the Fe_2O_3/FTO sensor was determined as 285 ^{o}C.

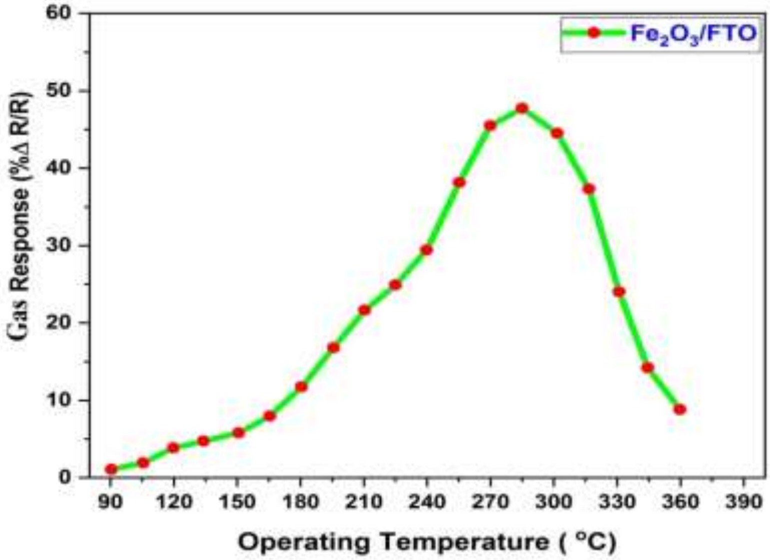

Figure 3.4. Sensitivity-operating temperature graph obtained from 100 ppm CO gas concentration of the Fe_2O_3/FTO sensor

The energy of the oxygen atoms sent to the surface increases with increasing temperature, which causes instability and inhibits the desired reaction with the target gas. Therefore, each of the sensor materials has a specific operating temperature.

In Figure 3.4, static gas measurements of the Fe_2O_3/FTO sensor as a function of temperature are given. The sensitivity of the sensor to constant 100 ppm CO gas at an operating temperature of 285 ^oC was 47.8%. It was observed that the sensitivity of the sensor decreased after 285 ^oC. After the operating temperature of 285 ^oC, a decrease in sensitivity was observed as the temperature increased. This decrease is observed for metal oxide semiconductor sensors. However, if the operating temperatures are too high, the O_2 molecules with enhanced activation can't reside on the Fe_2O_3 surface, thus preventing the formation of oxygen ions species (O^{-2}, O^- or O^{2-}_2). Little formed oxygen ions species was so strong disturbed by the desorption interaction that it can't return the conduction electron back to the sensors' conduction band. So the response value will decrease with the working temperature further increasing [12],[4],[13],[14] (Yang et al., 2015; Mirzaei et al., 2016; Wang et al., 2016; Liu et al., 2020).

(ii). Dynamic Gas Detection Results Based on Concentration

By making static gas detection measurement of the Fe_2O_3/FTO sensor, the optimum operating temperature was determined to be 285 °C. Dynamic gas measurements were carried out at an operating temperature of 285 ^{o}C and CO gas concentration varying between 5 ppm and 100 ppm. The dynamic gas measurement of the Fe_2O_3/FTO sensor is given in Figure 3.5. Also figure 3.6 shows the sensitivity-gas concentration graph of the Fe_2O_3/FTO sensor.

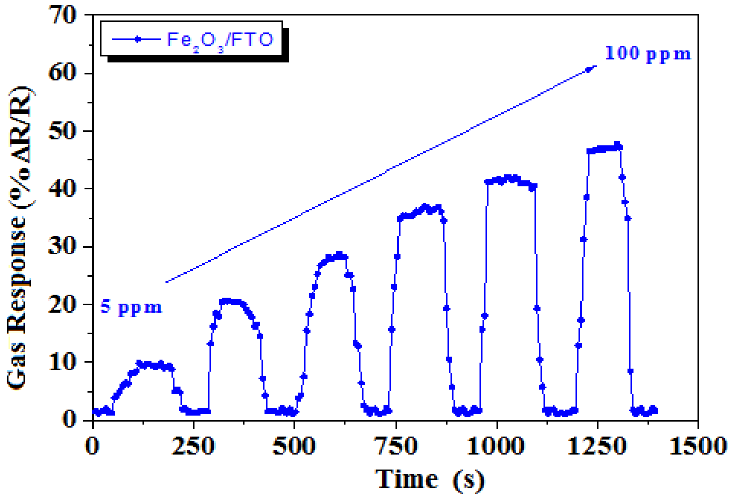

Fig 3.5. Dynamic gas measurement of the Fe_2O_3/FTO sensor at an operating temperature of 285 °C

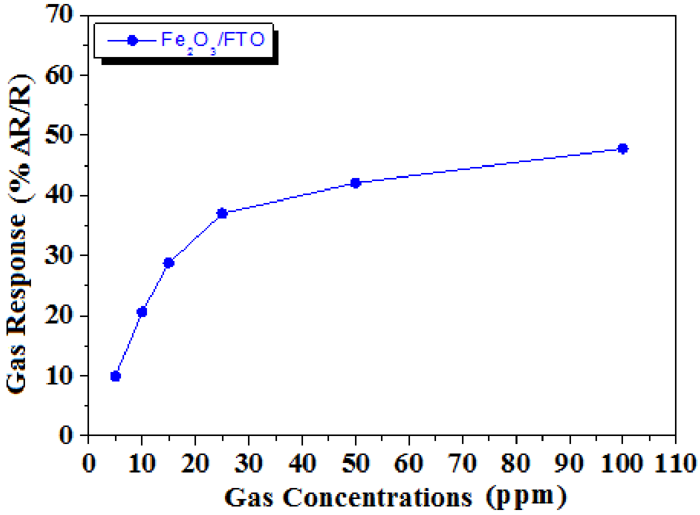

Figure 3.6. Sensitivity-gas concentration graph of Fe_2O_3/FTO sensor at 285 °C operating temperature

As seen in Figure 3.5 and Figure 3.6, it was observed that the sensitivity of the sensor increased as the CO gas concentration increased. This is because the sensing surface interacts with more target gas. With the increase of the CO gas concentration, the gas chemically reacts with more oxygen ion species on the sensing surface and more electrons are transferred back to α-Fe_2O_3 as a result of the reaction. This change increases the sensitivity of the sensor [4],[15],[16] (Mirzaei et al., 2016; Çorlu, 2017; Karaduman, 2017).

It was determined that the sensitivity of the Fe_2O_3/FTO sensor gradually increased when exposed to CO gas, and the sensitivity of the sensor returned to its initial values when the sensor surface was exposed to dry air. The sensitivity value of the sensor was determined as 10% for 5 ppm CO gas and 47.8% for 100 ppm CO gas. In Table 3.1, the sensitivity values of the Fe_2O_3/FTO sensor obtained under CO gas concentration between 5 ppm and 100 ppm are given.

Table 3.1. Dynamic gas detection measurement results of Fe_2O_3/FTO sensor at 285 °C operating temperature

Fe_2O_3/FTO Sensor	**SENSOR SENSITIVITY**					
	CO Gas Concentration					
	5 ppm	**10 ppm**	**15 ppm**	**25 ppm**	**50 ppm**	**100 ppm**
30 SILAR Cycle	10%	20.6%	28.8%	36.9%	42.1%	47.8%

(iii). Response and Recovery Times of Fe_2O_3/FTO Sensor

Response and recovery times of a gas sensor are basic parameters for gas detection applications. The sensor must detect the target gas quickly and remove the target gas from the sensing surface at the same rate. The response times of the Fe_2O_3/FTO sensor against 5 ppm-100 ppm CO gas concentrations at 285 °C operating temperature are shown in Figure 3.7, and the recovery times are shown in Figure 3.8.

The response times of the sensor for 5 ppm and 100 ppm CO gas concentrations were found to be 68 and 32 s, respectively. The recovery times for 5 ppm and 100 ppm CO gas concentrations were found to be 54 and 31 s, respectively.

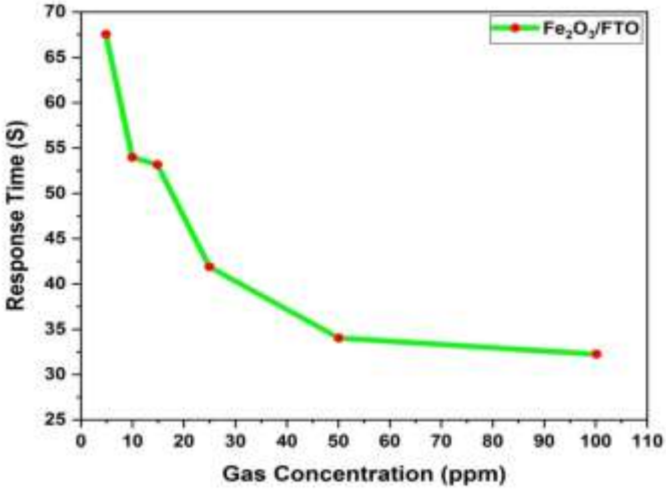

Figure 3.7. Fe_2O_3/FTO sensor response time vs gas concentration graph

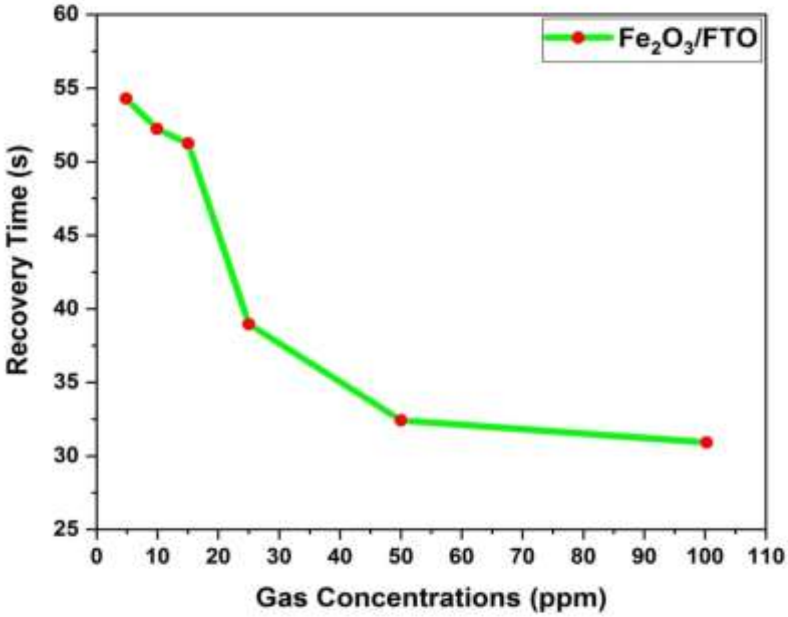

Figure 3.8. Fe_2O_3/FTO sensor recovery time vs gas concentration graph

(iv). Selectivity Gas Detection Results of Fe_2O_3/FTO Sensor

In general the selectivity is critical factor for a gas sensor. It describes the ability of a sensor to differentiate a specific target gas among other interfering gases. The selectivity of gas sensors should always be >1. A high selectivity corresponds to a higher response of the gas sensor to a target gas compared with the response to interfering gases. Typically, gas sensors are sensitive to more than one gas and exhibit cross-sensitivity. Hence, obtaining a high selectivity in a gas sensor is difficult, which limits the practical applications of gas sensors. Four common strategies for increasing the selectivity are (i) functionalization with noble-metal catalysts, (ii) tuning the sensing temperature, (iii) using heterojunctions and additives, and (iv) using filters **[1]**. Therefore, selectivity performance are the key factors for whether the sensor can be applied in practice. The selectivity (Q) can be defined according to Equation **[17]** :

$$\mathbf{Q} = \frac{R_{target\ gas}}{R_{interfering\ gas}} \qquad \mathbf{(3.4)}$$

It is well known that the high selectivity is an important factor for a reliable sensor. Figure 3.9 depicts the selectivity measurements of Fe_2O_3/FTO sensor to CO_2, CO, CH_4, NH_3, LPG and acetone gases. Under the operating conditions, our sensor demonstrated selective sensing to CO gas. Its response values for 100 ppm are about 21%, 47.8%, 6%, 2.5%, 15% and 4% for CO_2, CO, CH_4, NH_3, LPG and acetone gases, respectively. It can be seen that the sensor exhibited good selectivity to CO gas.

The Fe_2O_3/FTO thin film sensor shows better response to the CO gas and found that the sensor exhibits better response of 47.8% towards 100 ppm CO gas but its has small sensitive to other gases.

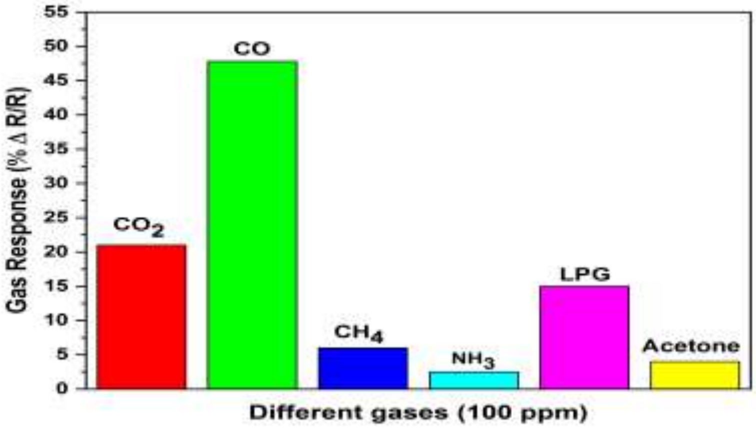

Figure 3.9. The comparison of responses of Fe_2O_3/FTO thin film sensor to various gases at 285 °C.

Fig. 3.9 shows that the sensor has a low gas response to other interfering gases except for CO, indicating a high specific adsorption capability for CO. The increased gas response to CO can be attributed to its superior electron-with drawing capabilities compared to other gases. According to the literature, the sensor's selectivity is determined by various factors, including the gas molecules' adsorption onto the sensor surface at varying temperatures and the target gas's LUMO (lowest unoccupied molecules orbit) energy **[18]**.

(v). Repeatability and Stability Gas Detection Results of Fe_2O_3/FTO Sensor

The repeatability and stability gas detection measurement results of the Fe_2O_3/FTO sensor at 285 ^{o}C operating temperature and 100 ppm CO gas concentration are given in Figure 3.10 and Figure 3.11, respectively.

In Figure 3.10, it is seen that the response and recovery characters of the sensor are very close to each other in each cycle and the response does not show a significant decrease, only very small fluctuations.

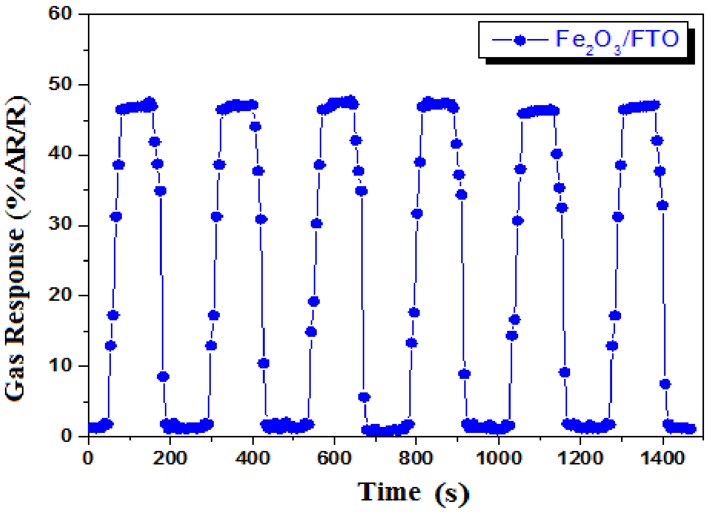

Figure 3.10. Repeatability graph of Fe_2O_3/FTO sensor

Stability refers to evaluating sensing performance data for at least one mouth. Generally, long-term operation of the sensor will increase the size of the sensing material particles, resulting in a slight decrease in the sensitivity **[19]**. Sensor materials that exhibit long-term stability without the need for constant replacement are essential for use in commercial applications. Therefore, production of gas sensing materials with longterm stability is of great importance from both commercial and scientific perspectives **[20]**. Therefore, we studied the long-term stability of our Fe_2O_3/FTO based gas sensor. **Fig. 3.11** shows the stability measurements for Fe_2O_3/FTO the sample. It can be seen that the sensor response to 100 ppm CO was almost constant during two months of continuous testing, suggesting that this sensor exhibit good long-term stability for CO detection. During the testing period only a slight the change in the sensitivity of the sensor was found to be 4%. This value shows that the sensor has long-term stability for detecting CO gas. The slight decrease in the gas response is attributed to the formation of a moisture or oxide layer. It should be noted that the adsorption of CO molecules on the surface of the gas sensor is one possible reason for decrease of the response. Water molecules reduce the number of the available sites for gas adsorption, decreasing the sensitivity **[21]**.

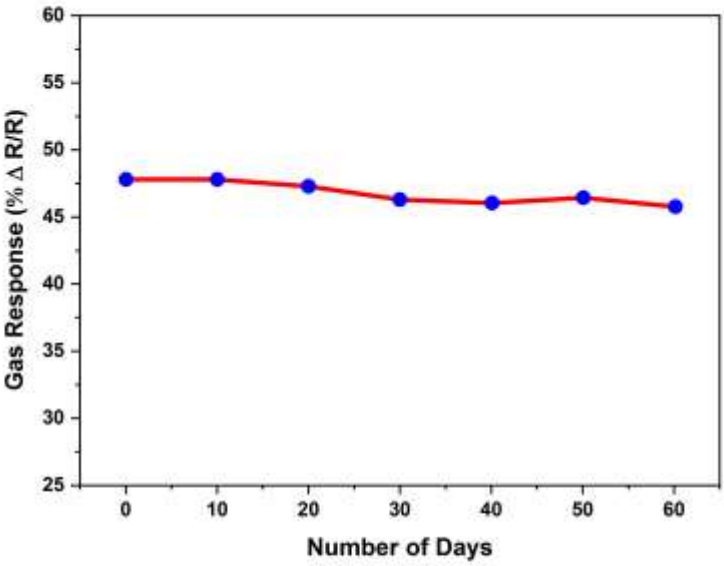

Fig. 3.11 The Fe_2O_3/FTO sample's stability against 100 ppm CO at an operating temperature of 285 °C.

4. CONCLUSIONS

The SILAR method was successfully deposited Fe_2O_3 thin film for CO gas sensor application. Fe_2O_3 gas sensors demonstrated outstanding CO sensing features at variance concentrations of 5–100 ppm at operating temperatures of 285 C. The characterizations of X-ray diffraction (XRD), Scanning electron microscope (SEM), Energy dispersive X-ray analyzer (EDAX) and gas measurement systems for the analysis of structural, morphological, chemical component and gas sensing properties of Fe_2O_3 thin film were carried. It also can be concluded that silver electrodes Ag has a significant effect on the sensing parameters of Fe_2O_3 film and that SILAR is an appropriate approach in developing thin films for gas sensing applications.

References

[1] Mirzaei, A., Lee, J. H., Majhi, S. M., Weber, M., Bechelany, M., Kim, H. W., & Kim, S. S. (2019). Resistive gas sensors based on metal-oxide nanowires. *Journal of Applied Physics*, *126*(24), 241102.

[2] Pearton, S. J., Ren, F., Wang, Y. L., Chu, B. H., Chen, K. H., Chang, C. Y. ... and Norton, D. P. (2010) “Recent advances in wide bandgap semiconductor biological and gas sensors”, ***Progress in Materials Science***, 55(1), 1-59.

[3] Ma, Y., Xie, X. Y., Chen, H. Y., Zhang, T. H. and Debela, T. T. (2021) “The growth mode of α-Fe_2O_3 thin films by DC magnetron sputtering”, ***Vacuum***, 194, 110625.

[4] Mirzaei, A., Hashemi, B. and Janghorban, K. (2016) “α-Fe_2O_3 based nanomaterials as gas sensors”, ***Journal of Materials Science: Materials in Electronics***, 27(4), 3109-3144.

[5] I. Karaduman, E. Er, H. Eelikkan, S. Acar, A new generation gas sensing material based on high-quality graphene. Sens. Actuators B 221, 1188–1194 (2015)

[6] Fareed, S. S., Mythili, N., Vijayaprasath, G., Chandramohan, R. and Ravi, G. (2018) “α-Fe_2O_3 nanoparticles as a byproduct from the thin film (SILAR) deposition process: a study on the product”, ***Materials Today: Proceedings***, 5(10), 20955-20965.

[7] Khakpour, Z., Pourfarahani, H., Maghsoudipour, A., and Ebadzadeh, T. (2018) “Synthesis and deposition of hematite nanoparticles on Fluorine-doped Tin Oxide (FTO) glass substrates”, ***Materials Today: Proceedings***, 5(7), 15828-15835.

[8] Rahman, G., Najaf, Z., and Mian, S. A. (2020) “Investigation of the structural, optical, and photoelectrochemical properties of α-Fe_2O_3 nanorods synthesized via a facile chemical bath deposition”, ***Optik*****,** 200**,** 163454.

[9] Machreki, M., Chouki, T., Martelanc, M., Butinar, L., Vodopivec, B. M. and Emin, S. (2021) “Preparation of porous α-Fe_2O_3 thin films for efficient photoelectrocatalytic degradation of basic blue 41 dye”, ***Journal of environmental chemical engineering***, 9(4), 105495.

[10] Choi, Y., Lee, H., Kumbhar, V. S., Choi, Y. W., Kim, J. and Lee, K. (2020) “Enhancement of photoelectrochemical properties with α–Fe_2O_3 on surface modified FTO substrates”, ***Ceramics International***, 46(12), 20012-20019.

[11] Júnior, J. W. N., Monção, R. M., Bandeira, R. M., dos Santos Júnior, J. R., Araujo, J. F. D. F., Moura, J. V. B. ... and de Sousa, R. R. M. (2021) “Growth of α-Fe_2O_3 thin films by plasma deposition: Studies of structural, morphological, electrochemical, and thermal-optical properties”, ***Thin Solid Films***, 736, 138919.

[12] Yang, F. and Guo, Z. (2015). “Comparison of the enhanced gas sensing properties of tin dioxide samples doped with different catalytic transition elements”, ***Journal of Colloid and İnterface Science***, 448, 265-274.

[13] Wang, C., Zeng, W., Luo, L., Zhang, P. and Wang, Z. (2016) “Gas-sensing properties and mechanisms of Cu-doped SnO_2 spheres towards H_2S”, ***Ceramics International***, 42, 10006-10013.

[14] Liu, L., Fu, S., Lv, X., Yue, L., Fan, L., Yu, H. ... and Zhu, W. (2020) “A gas sensor with Fe_2O_3 nanospheres based on trimethylamine detection for the rapid assessment of spoilage degree in fish”, ***Frontiers in Bioengineering and Biotechnology***, 1120.

[15] Çorlu, T., Karaduman, I., Yildirim, M. A., Ateş, A. and Acar, S. (2017) “Effect of doping materials on the low-level NO gas sensing properties of ZnO thin films”, ***Journal of Electronic Materials***, 46 (7), 3995-4002.

[16] Karaduman, I., Yıldırım, M. A., Yıldırım, S. T., Ateş, A., Özdemir, Y. A. and Acar, S. (2017) “The effect of different doping elements on the CO gas sensing properties of ZnO nanostructures”, ***Journal of Materials Science: Materials in Electronics***, 28 (23), 18154-18163.

[17] Liu, J., Zhang, L., Fan, J., & Yu, J. (2022). Semiconductor gas sensor for triethylamine detection. *Small*, *18*(11), 2104984.

[18] Rzaij, J. M., & Habubi, N. F. (2022). Enhancing the CO_2 sensor response of nickel oxide-doped tin dioxide thin films synthesized by SILAR method. *Journal of Materials Science: Materials in Electronics*, 1-13.

[19] Bai, X., Lv, H., Liu, Z., Chen, J., Wang, J., Sun, B., ... & Shi, K. (2021). Thin-layered MoS_2 nanoflakes vertically grown on SnO_2 nanotubes as highly effective room-temperature NO_2 gas sensor. *Journal of Hazardous Materials*, *416*, 125830.

[20] Zhang, D., Liu, J., & Xia, B. (2016). Nitrogen dioxide-sensing properties at room temperature of metal oxide-modified graphene composite via one-step hydrothermal method. *Journal of Electronic Materials*, *45*(8), 4324-4330.

[21] Bang, J. H., Mirzaei, A., Han, S., Lee, H. Y., Shin, K. Y., Kim, S. S., & Kim, H. W. (2021). Realization of low-temperature and selective NO_2 sensing of SnO_2 nanowires via synergistic effects of Pt decoration and Bi_2O_3 branching. *Ceramics International*, *47*(4), 5099-5111.